Journal of Electroceramics, 15, 151–157, 2005

Thick Film Planar CO_2 Sensors Based on Na β-Alumina Solid Electrolyte

HYUN SEOK HONG,[1,*] JUN WOONG KIM,[1] SANG JIN JUNG[2] & CHONG OOK PARK[1]

[1]*Department of Materials Sci. & Engineering, Korea Advanced Institute of Science and Technology, 373-1, Guseong-Dong, Yuseong-Gu, Daejon, 305-701, South Korea*

[2]*Electronic Ceramics Center, Dong-Eui University, 995 Eomgwangno, Busanjin-gu, Busan, 614-714, South Korea*

Submitted November 4, 2004; Revised March 24, 2005

Abstract. Practical small-sized thick film CO_2 sensor with self-heater was fabricated with Na β-Alumina (NBA), $Na_2Ti_6O_{13}$-TiO_2, and Na_2CO_3 as a solid electrolyte, reference electrode, and a sensing electrode, respectively. The measured EMF from the sensor followed the Nernstian behavior with CO_2 concentration change in the range of 400 to 600°C (350–580 mW power consumption). However, in the aspect of stability, densification of the NBA thick film and prevention of Na_2CO_3 evaporation were needed. In this study, an Al_2O_3 porous layer deposited on Na_2CO_3 was effective in improving the durability during operation of the sensor. It is thought that Al_2O_3 suppresses evaporation of Na_2CO_3.

Keywords: thick film, self-heater, CO_2 sensor, NBA, evaporation

1. Introduction

CO_2 monitoring is important in various fields such as bio-related engineering, chemical plant, food industry, medical system, indoor air quality and others. A conventional Non Distributive Infra Red (NDIR) absorption CO_2 detector is expensive, large in volume, and vulnerable to contamination in spite of its high precision. Therefore, cheap and compact electrochemical CO_2 sensors are in high demand. Electrochemical potentiometric CO_2 sensors using solid electrolytes are most promising among the various methods for the detection of carbon dioxide because of their compact structure, high selectivity, low cost, and the ability of continuous monitoring.

There have been a number of works on electrochemical CO_2 sensors with type III potentiometric design for various combinations of solid electrolytes, and electrodes (sensing, reference) [1–4, 7–9]. In the level of laboratory experiment, they showed satisfactory CO_2 sensing characteristics including fast response, high sensitivity, and excellent selectivity.

*To whom all correspondence should be addressed. E-mail: hhs5798@kaist.ac.kr

However, those CO_2 sensors were prepared as bulky type based on sintered ceramic electrolyte pellets and they were heated by the outer electrical furnace. Also, regarding the structure of sensor, sandwich type cells based on a solid electrolyte layer between two electrodes must be disadvantageous in mass production.

Screen printing method has been attractive in its ability of low cost mass-production and in its capability to give better uniformity in the final device's properties [5]. Thick film devices based on the screen printing method are also characterized by low power consumption. In this work, a thick film planar CO_2 sensor with self heater was fabricated on the alumina substrate using a screen printing technique to realize a small practical CO_2 sensor and its sensing characteristics were evaluated. The electrochemical cell, O_2, CO_2, Au/Na_2CO_3//NBA//$Na_2Ti_6O_{13}$-TiO_2, Au, O_2 was basically the same as those of Holzinger et al. [7–9].

2. Experimental

2.1. CO_2 Sensor Preparation

To synthesize Na-beta alumina solid electrolytes, Na_2CO_3 (Aldrich) and Al_2O_3 (Aldrich) powders were

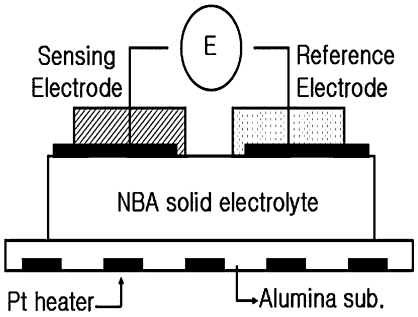

Fig. 1. Schematic structure of the thick film CO_2 sensor.

weighed in a molar ratio of 1:11 and wet-milled in a zirconia ball-containing bottle. The resulting powder was dried, ground, and heat treated at 1300°C for one day and identified by X-ray diffraction. As a reference, a $Na_2Ti_6O_{13}$–TiO_2 mixture was prepared by heating a mixture of Na_2CO_3 and TiO_2 (1:6 molar ratio) at 1050°C for 24 hours [6, 9]. Na_2CO_3 powder was used as auxiliary phase. All the powders were transformed into screen printable pastes by mixing them with organic binder. Figure 1 shows the schematic structure of the prepared sensor.

Overall dimensions of the fabricated sensors were 0.2 mm thickness, 2.5 mm width, and 2.5 mm length. Firstly, NBA paste was printed on the alumina substrate and fired at 1300–1600°C for 1 hour. On the back of the substrate, Pt paste for the heater was screen-printed and heat-treated at 1000°C for 1 hour.

Then, Au paste was deposited on the designated region of the NBA film as electrodes for the EMF signal, and $Na_2Ti_6O_{13}$-TiO_2 paste was covered on one Au electrode before they were baked at 900°C in air together. Na_2CO_3 was painted on the other Au electrode and baked at 700°C for 30 minutes. A view of the sensing element is shown in Fig. 2.

Finally, Pt wires were attached with Au paste on two electrode pads and on two Pt heater pads on the back side of substrate. Four wires from sensing element were connected to packaging can with silver paste. This packaged sensor was loaded on the small gas chamber with a gas inlet and a gas outlet. To energize the sensor, appropriate heater voltage was controlled by D.C. power supply. EMF of the sensor was measured with Keithly 617 high impedance electrometer interfaced with a PC. Different CO_2 concentrations were achieved by diluting three different gases (1% CO_2 with an N_2 balance, 100% O_2, and 100% N_2) with a gas mixer

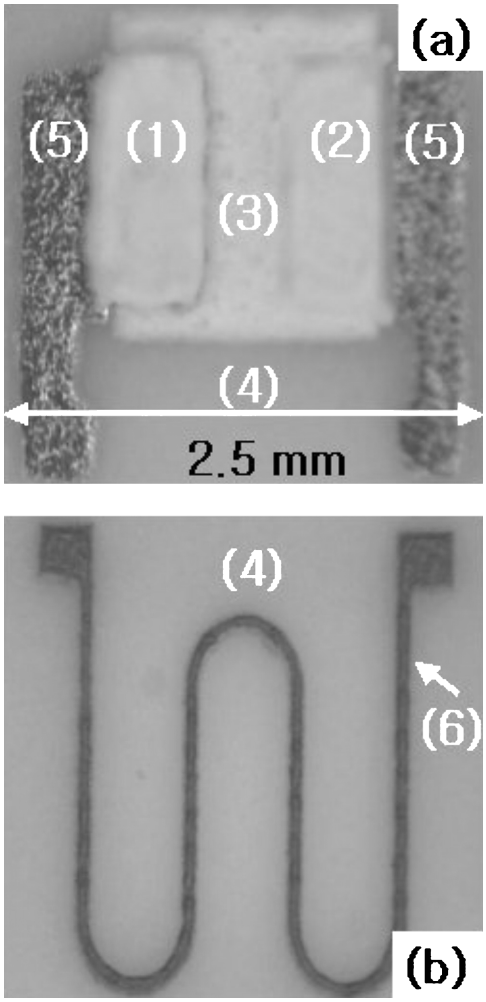

Fig. 2. Photographs of the fabricated thick film CO_2 sensor (a) A Top view [(1) Na_2CO_3 sensing electrode, (2) $Na_2Ti_6O_{13}$-TiO_2/Au reference electrode, (3) NBA electrolyte, (4) Al_2O_3 substrate, (5) Au electrode] (b) Bottom view [(4) Al_2O_3 substrate, (6) Pt heater].

connected to a precision gas flow controller. The total gas flow rate was 0.2 L/min.

2.2. *CO_2 Sensing Mechanism*

When the following electrochemical cell (1) is constructed, the EMF E can be expressed by the difference of the chemical potentials μ of Na (or the activities a of Na) on both sides (I = sensing electrode/solid electrolyte interface, II = reference electrode/solid electrolyte interface) of the cell as in Eq. (2) as other

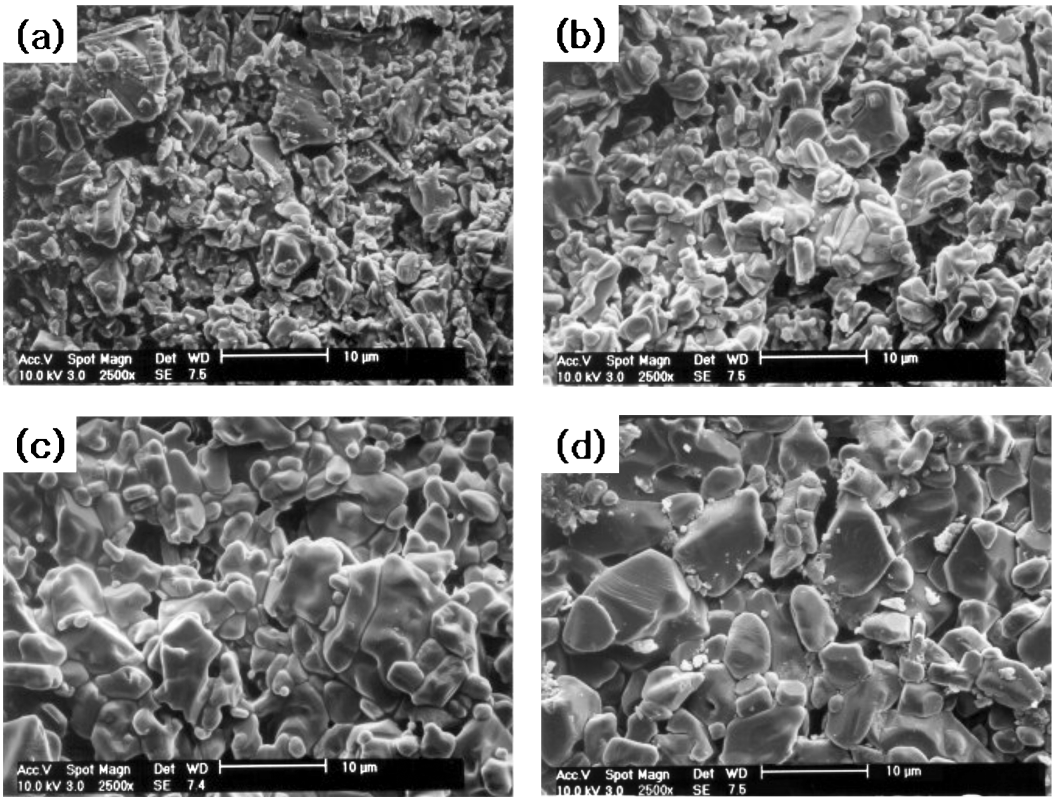

Fig. 3. SEM photographs of NBA films sintered at (a) 1300°C (b) 1400°C (c) 1500°C and (d) 1600°C for 1 hour in air.

researches reported [7, 9].

$$\mathrm{Au}, O_2, CO_2, Na_2CO_3|Na^+|Na_2Ti_6O_{13} - TiO_2, O_2, \mathrm{Au} \quad (1)$$

$$E = -\frac{1}{F}\left(\mu^{\mathrm{II}}_{\mathrm{Na}} - \mu^{\mathrm{I}}_{\mathrm{Na}}\right) = -\frac{RT}{F}\ln\left(\frac{a^{\mathrm{II}}_{\mathrm{Na}}}{a^{\mathrm{I}}_{\mathrm{Na}}}\right) \quad (2)$$

where the magnitude of $a^{\mathrm{I}}_{\mathrm{Na}}$, and $a^{\mathrm{II}}_{\mathrm{Na}}$ is determined by the following chemical reactions (3) and (4).

$$Na_2CO_3 \leftrightarrow 2\mathrm{Na} + 1/2O_2 + CO_2 \quad (3)$$

$$2\mathrm{Na} + 6TiO_2 + 1/2O_2 \leftrightarrow Na_2Ti_6O_{13} \quad (4)$$

Therefore, $a^{\mathrm{I}}_{\mathrm{Na}}$ and $a^{\mathrm{II}}_{\mathrm{Na}}$ are expressed by the following equations.

$$\ln a^{\mathrm{I}}_{\mathrm{Na}} = -\frac{\Delta_f \mathrm{G}^{\circ}_{\mathrm{Na_2CO_3}} - \Delta_f G^{\circ}_{\mathrm{CO_2}}}{2RT} - \frac{1}{2}\ln P^{\mathrm{I}}_{\mathrm{CO_2}} - \frac{1}{4}\ln P^{\mathrm{I}}_{\mathrm{O_2}} \quad (5)$$

$$\ln a^{\mathrm{II}}_{\mathrm{Na}} = -\frac{\Delta_f \mathrm{G}^{\circ}_{\mathrm{Na_2Ti_6O_{13}}} - 6\Delta_f G^{\circ}_{\mathrm{TiO_2}}}{2RT} - \frac{1}{4}\ln P^{\mathrm{II}}_{\mathrm{O_2}} \quad (6)$$

The overall cell reaction (7) is obtained by combining the anodic side reaction (3) with the cathodic side reaction (4). Consequently, the EMF is expressed as in Eq. (8)

$$Na_2CO_3 + 6TiO_2 \leftrightarrow Na_2Ti_6O_{13} + CO_2 \quad (7)$$

$$E = -\frac{\Delta_R G}{2\mathrm{F}} = -\frac{\Delta_R G^{\circ}}{2\mathrm{F}} - \frac{RT}{2F}\ln\frac{P_{\mathrm{CO_2}}}{P^{\circ}} \quad (8)$$

where $\Delta_R G^{\circ} = \Delta_f G^{\circ}_{\mathrm{Na_2Ti_6O_{13}}} + \Delta_f G^{\circ}_{\mathrm{CO_2}} - \Delta_f G^{\circ}_{\mathrm{Na_2CO_3}} - 6\Delta_f G^{\circ}_{\mathrm{TiO_2}}$ Since $P^{I}_{\mathrm{O_2}} = P^{\mathrm{II}}_{\mathrm{O_2}} = P_{O_2}$ in this open reference cell [7, 9], the oxygen partial pressure has no influence on the EMF.

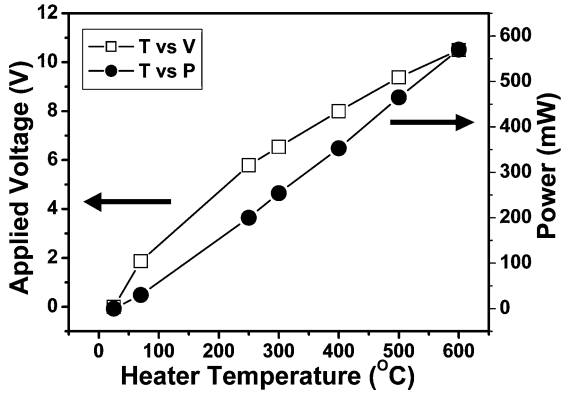

Fig. 4. Characteristics of the Pt local heater.

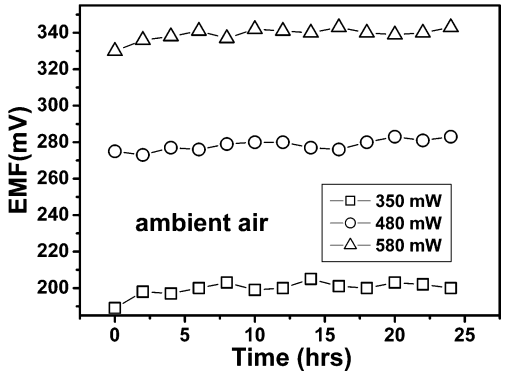

Fig. 5. EMF of the thick film CO_2 sensor in ambient air at various power consumptions.

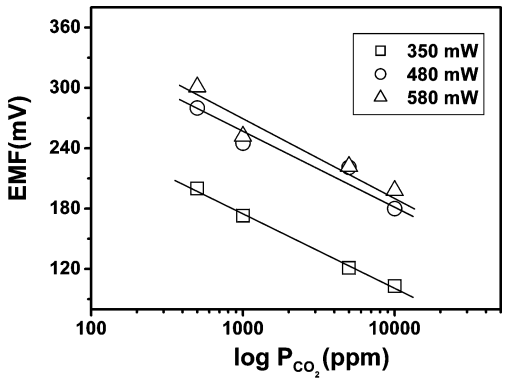

Fig. 6. EMF vs. log P_{CO_2} of the thick film CO_2 sensor at various power consumptions.

3. Results and Discussion

As shown in Fig. 3, screen-printed NBA electrolyte film was more densified with increasing sintering temperature from 1300 to 1600°C. At 1300°C, the NBA film was hardly densified. However, above 1400°C, alumina substrate was also sintered and became bent. Therefore, the NBA film was fired at 1400°C for 1 hour for all cases. The thickness of NBA electrolyte and Au electrode were about 40 μm and 20 μm, respectively. To obtain enough thickness of the electrolyte, NBA paste was printed several times.

To relate the applied voltage of the Pt heater to temperature, the resistance of the Pt heater was measured versus temperature and versus the applied dc voltage. The characteristic of the Pt heater is shown in Fig. 4. As can be seen from Fig. 4, in order to fix the Pt heater temperature as 400–600°C, the applied dc voltage to heater had to be fixed between 8 V and 10.5 V. Of course, the temperature of the heater is always not identical to that of the sensor. This means that heat-transfer from the heater to the sensor through the alumina substrate should be considered. In this work it is assumed that the heater and the sensor become isothermal on power application. Prepared sensors showed reproducible and satisfactory sensing characteristics to gases of different CO_2 content at 350–580 mW. Prior to observing CO_2 response of the sensor, the sensor was heated for 24 hours in ambient air which contained humidity, CO_2, O_2. As shown in Fig. 5, stable EMF values were obtained at 350–580 mW in ambient air. Response time was a few minutes to reach 90% value of the equilibrium EMF while Holzinger et al. [7–9] observed a few seconds of response time in their CO_2 sensors. Such a difference in response time is thought to be due to the difference in time needed for determined composition of gases to be saturated in the whole gas chambers where sensors are loaded.

Sensitivity were 74 mV/dec. at 350 mW, 65 mV/dec. at 480 mW and 67 mV/dec. at 580 mW as shown in Fig. 6. This values showed significant discrepancy with the theoretical values [66.7 mV/dec. at 350 mW (400°C), 76.6 mV/dec. at 480 mW (500°C), 86.5 mV/dec. at 580 mW (600°C)]. We believe that this discrepancy in sensitivity originates from the error in temperature. Nevertheless, E vs. log P_{CO2} shows a linear relationship obeying the Nernst law for all the cases.

Figure 7 shows the stability of the sensor at various values of the operating power. If the life-time of the sensor is defined as the time until the sensor EMF begins to deviate from the original value by 10%, the life-time of the prepared CO_2 sensor was 3 days at 580 mW, 4 days at 480 mW, and 7 days at 350 mW.

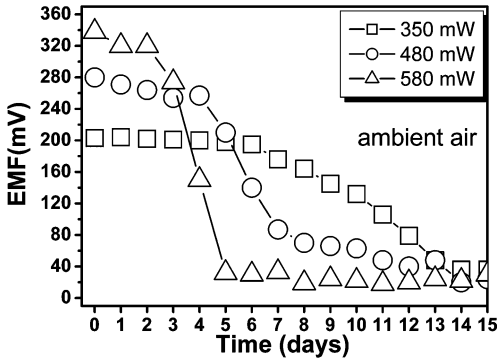

Fig. 7. Signal durability of the thick film CO_2 sensor in ambient air at various power consumptions.

The stability of the sensor seems to be related to operation temperature, i.e, at higher operation temperature, shorter durability of the sensor was observed. Figure 8 shows the tendency of evaporation of sodium carbonate with time at 480 mW power consumption. The Na_2CO_3 layer on the Au electrode gradually evaporated with operation time of the sensor as shown in Fig. 8. Although the melting point of Na_2CO_3 is about 845°C, it began to evaporate gradually at 400°C [10]. Furthermore, a high ratio of the surface area to the thickness of the Na_2CO_3 film accelerated the evaporation. After continuous evaporation of Na_2CO_3, only Au electrode finally remained. Evaporation of the Na_2CO_3 auxiliary phase on the Au electrode may give rise to reduction of triple phase junction area where CO_2-O_2 gas, Na^+ ions and electrons equilibrate electrochemically at the sensing electrode. However, complete exhaustion of Na_2CO_3 did not likely occur and moreover, the relationship between the amount of Na_2CO_3 and the EMF could not be explained clearly. The change of the microstructure or the adhesion property of homoionic junction (between Na^+ conductor, NBA, and poor Na^+ conductor, Na_2CO_3 auxiliary phase) followed by Na_2CO_3 evaporation may be the another reason of the

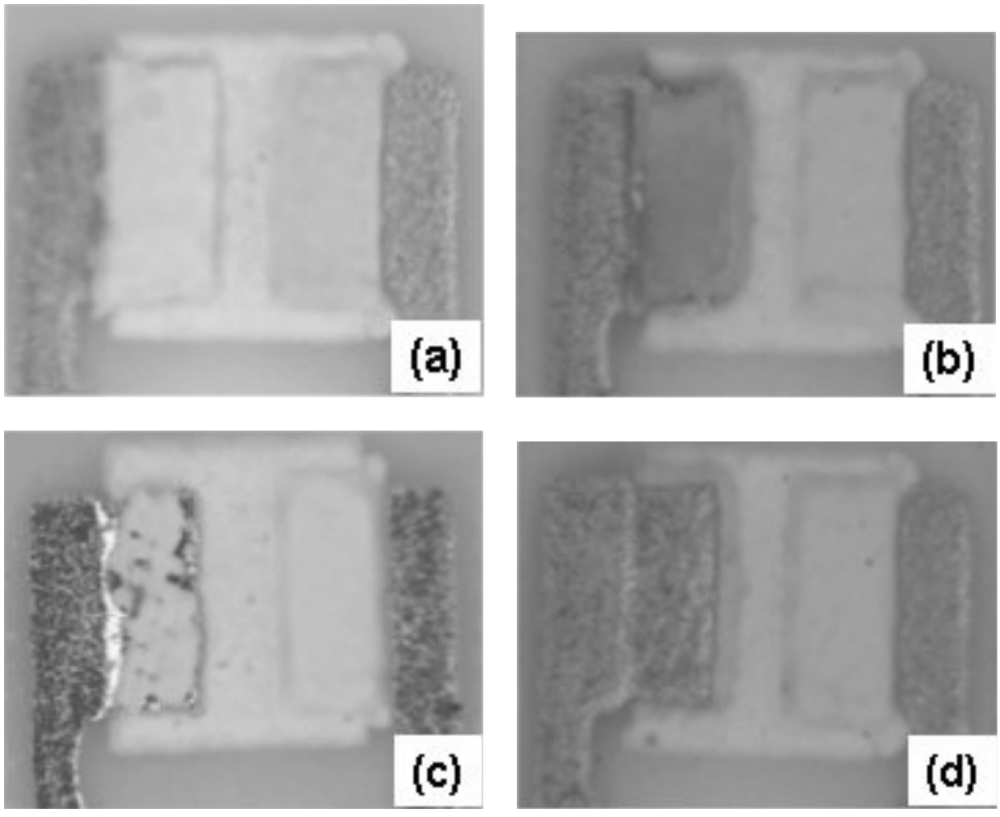

Fig. 8. Evaporation of Na_2CO_3 electrode with operation time of (a) before experiment, (b) 1 day, (c) 3 days, and (d) 7 days at 480 mW power consumption.

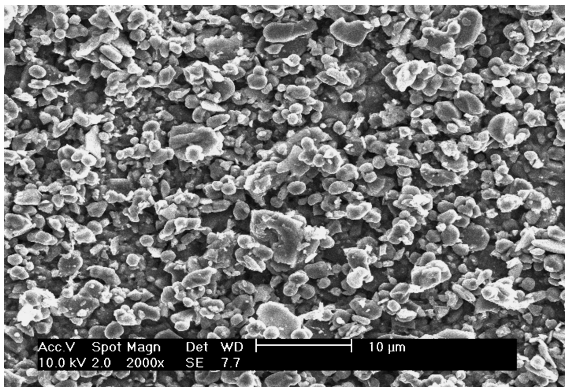

Fig. 9. SEM photograph (A Top view) of the Al_2O_3 additive layer on Na_2CO_3.

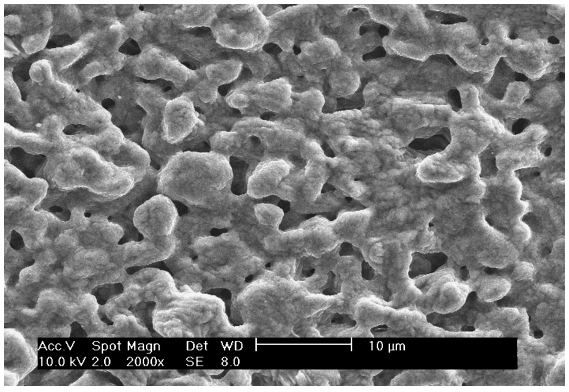

Fig. 10. SEM photograph (A Top view) of the Na_2CO_3 layer sintered at 700°C for 30 minutes.

EMF degradation caused by Na_2CO_3 evaporation with duration time.

In this study, an α-Al_2O_3 additive layer was deposited on Na_2CO_3 which had been baked at 700°C for 30 minutes previously and fired at 700°C for another 30 minutes together resulting in a Al_2O_3/Na_2CO_3/Au multi-layer structure of the sensing electrode. Alumina paste was formulated by mixing Al_2O_3 (Aldrich) powder thoroughly with SiO_2-Al_2O_3-B_2O_3 based glass frit, ethylcellulose, and α-terpineol for 1 hour. Figure 9 shows the final microstructure of the Al_2O_3 additive layer on the sodium carbonate in the CO_2 sensor. Na_2CO_3 as a single auxiliary phase sintered 700°C for 30 minutes was shown for comparison in Fig. 10.

In order to increase the stability of the auxiliary electrode, Miura et al. [11–13] extensively modified the pure Na_2CO_3 by mixing with $BaCO_3$, $CaCO_3$ and

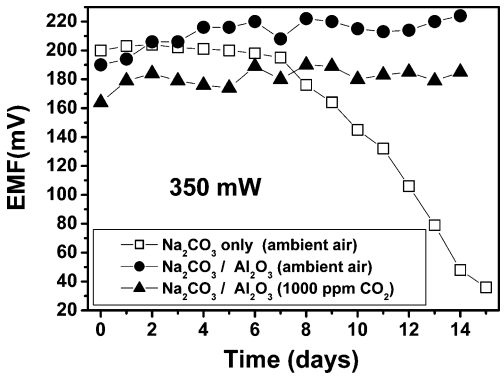

Fig. 11. Improved stability of the thick film CO_2 sensor with Al_2O_3/Na_2CO_3 sensing electrode.

$SrCO_3$ since these compounds are known to be highly resistive to water vapor in the ambient due to their very low solubility in water. However, such binary carbonates are focused on the increment of humidity resistance in the auxiliary electrode. Moreover, there is a report [14] that co-existence of $BaCO_3$ accelerates the volatility of Na_2CO_3.

As shown in Fig. 11, a sensor with an Al_2O_3/Na_2CO_3/Au multi-layer sensing electrode showed reproducible EMF with CO_2 changes (1000 ppm CO_2 to air) during 15 days although a little E^O value shift (average: +2 mV/day) was observed.

Moreover, the sensor with the Al_2O_3/Na_2CO_3 sensing electrode showed almost the same sensitivity (about 70 mV/dec.) and response time as the sensor with the pure Na_2CO_3 sensing electrode. This implies that Al_2O_3 was not only porous but also did not alter the electrochemical reaction at the sensing electrode. It is thought that improved stability came from the suppressing effect of alumina layer on evaporation of Na_2CO_3.

4. Conclusions

Very small (2.5 mmW × 2.5 mmL × 0.2 mm T) thick film CO_2 sensors with self-heater were fabricated using a screen printing method. In the power range of 350–580 mW, the sensors showed a logarithmic dependency of the EMF on CO_2 partial pressure change. A porous Al_2O_3/Na_2CO_3 double layer sensing electrode resulted in a more stable long term characteristics, which may be related to the suppression of evaporation of Na_2CO_3

on the Au electrode with the aid of an Al_2O_3 protective layer. The high sintering temperature of Na-beta alumina makes it difficult to achieve high density electrolyte films.

Acknowledgments

This research was funded by the Center for Ultramicrochemical Process Systems sponsored by KOSEF.

References

1. N. Yamazoe, S. Hosohara, T. Fukuda, K. Isono, and N. Miura, *Sensors and Actuators B*, **34**, 361 (1996).
2. H. Aono, E. Sugimoto, Y. Sadaoka, N. Imanaka, and G. Adachi, *J. Electrochem. Soc*., **136**, 590 (1989).
3. N. Imanaka, T. Kawasato, and G. Adachi, *CHEMISTRY LETTERS*, 497 (1990).
4. H. Näfe, *J. Electrochem. Soc*., **144**, 915 (1997).
5. Ceramic Materials for Electronics: Processing, Properties and Application, Edited by Relva C, Buchanan, Marcel Dekker, Inc. (1991) p. 435–488.
6. S. Andersson and A. D. Wadsley, *Acta Cryst.*, **15**, 194.
7. M. Holzinger, J. Maier, and W. Sitte, *Solid State Ionics*, **94**, 217 (1997).
8. J. Maier, M. Holzinger, and W. Sitte, *Solid State Ionics*, **74**, 5 (1994).
9. M. Holzinger, J. Maier, and W. Sitte, *Solid State Ionics*, **86–88**, 1055 (1996).
10. H.-H. Möbius, *J. Solid State Electrochem.* **8**, 94 (2004).
11. N. Miura, S. Yao, Y. Shimizu, and N. Yamazoe, *Sensors and Actuators* B, **9**, 165 (1992).
12. N. Miura, S. Yao, Y. Shimizu, and N. Yamazoe, *J. Electrochem. Soc*., **139**, 1384 (1992).
13. S. Yao, Y. Shimizu, N. Miura, and N. Yamazoe, *CHEMISTRY LETTERS*, 2033 (1990).
14. Brosda S. (1992) Thesis, University of Greifswald.